AD-A188 187 FUNDAMENTAL CYCLOTRON FREQUENCY GENERATION FROM A CUSPTRON OSCILLATOR(U) NAVAL SURFACE WEAPONS CENTER SILVER SPRING MD W NAMKUNG ET AL. 01 AUG 87 1/1

UNCLASSIFIED NSWC/TR-87-268 F/G 9/1 NL

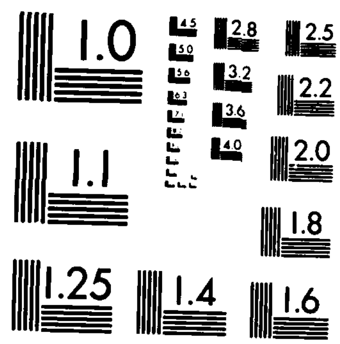

MICROCOPY RESOLUTION TEST CHART
NATIONAL BUREAU OF STANDARDS-1963-A

DTIC FILE COPY

4

NSWC TR 87-268

AD-A188 187

FUNDAMENTAL CYCLOTRON FREQUENCY GENERATION FROM A CUSPTRON OSCILLATOR

BY W. NAMKUNG J. Y. CHOE H. S. UHM V. AYRES

RESEARCH AND TECHNOLOGY DEPARTMENT

1 AUGUST 1987

Approved for public release; distribution is unlimited.

NAVAL SURFACE WARFARE CENTER

Dahlgren, Virginia 22448-5000 • Silver Spring, Maryland 20903-5000

REPORT DOCUMENTATION PAGE

1a REPORT SECURITY CLASSIFICATION UNCLASSIFIED	1b RESTRICTIVE MARKINGS AD-A188 187
2a SECURITY CLASSIFICATION AUTHORITY	3 DISTRIBUTION/AVAILABILITY OF REPORT Approved for public release; distribution is unlimited.
2b DECLASSIFICATION/DOWNGRADING SCHEDULE	
4 PERFORMING ORGANIZATION REPORT NUMBER(S) NSWC TR 87-268	5 MONITORING ORGANIZATION REPORT NUMBER(S)
6a NAME OF PERFORMING ORGANIZATION Naval Surface Warfare Center 6b OFFICE SYMBOL (If applicable) R43	7a NAME OF MONITORING ORGANIZATION
6c ADDRESS (City, State, and ZIP Code) White Oak Laboratory 10901 New Hampshire Avenue Silver Spring, MD 20903-5000	7b ADDRESS (City, State, and ZIP Code)
8a NAME OF FUNDING/SPONSORING ORGANIZATION 8b OFFICE SYMBOL (If applicable)	9 PROCUREMENT INSTRUMENT IDENTIFICATION NUMBER
8c ADDRESS (City, State, and ZIP Code)	10 SOURCE OF FUNDING NUMBERS PROGRAM ELEMENT NO 61152N PROJECT NO RR00001 TASK NO RR01109 WORK UNIT ACCESSION NO

11 TITLE (Include Security Classification)
Fundamental Cyclotron Frequency Generation From A Cusptron Oscillator

12 PERSONAL AUTHOR(S) Namkung, W., Choe, J. Y., Uhm, H. S., Ayers, V.

13a TYPE OF REPORT	13b TIME COVERED	14 DATE OF REPORT (Year, Month, Day)	15 PAGE COUNT
Final	FROM ____ TO ____	1987, August, 01	20

16 SUPPLEMENTARY NOTATION

17 COSATI CODES			18 SUBJECT TERMS (Continue on reverse if necessary and identify by block number)
FIELD	GROUP	SUB GROUP	Microwave Generation ;
09	01,03		Fundamental Cyclotron Frequency
20	07		Cusptron Oscillation

19 ABSTRACT (Continue on reverse if necessary and identify by block number)

The first experiment is reported for microwave generation of the fundamental electron cyclotron frequency from a cusptron oscillator with a smooth conducting wall. A non-relativistic axis-rotating electron beam is used to generate the TE_{11} circular modes in a cavity by the negative mass instability. The TE_{111} and TE_{112} modes are separately excited without any mode competition at an appoximately 1.8 kW output power with 7.8 percent efficiency.

20 DISTRIBUTION/AVAILABILITY OF ABSTRACT ☒ UNCLASSIFIED/UNLIMITED ☐ SAME AS RPT ☐ DTIC USERS	21 ABSTRACT SECURITY CLASSIFICATION UNCLASSIFIED
22a NAME OF RESPONSIBLE INDIVIDUAL W. Namkung	22b TELEPHONE (Include Area Code) (202) 394-2556 22c OFFICE SYMBOL R43

DD FORM 1473, 84 MAR 83 APR edition may be used until exhausted. All other editions are obsolete.

SECURITY CLASSIFICATION OF THIS PAGE

☆ U.S. Government Printing Office: 1986 — 607-044

FOREWORD

The first experiment is reported for microwave generation at the fundamental electron cyclotron frequency from a cusptron oscillator with a smooth conducting wall. A non-relativistic axis-rotating electron beam is used to generate the TE_{11} circular modes in a cavity by the negative mass instability. The TE_{111} and TE_{112} modes are separately excited without any mode competition at approximately 1.8 kW output power with 7.8 percent efficiency. We are grateful to K. Allen and W. Grine for their technical assistance. This work was supported in part by the Independent Research Fund at the Naval Surface Weapons Center and in part by the Office of Innovative Science and Technology of the Strategic Defense Initiative Organization managed by the Harry Diamond Laboratories.

Approved by:

Carl W. Larson

CARL W. LARSON, Head
RADIATION DIVISION

CONTENTS

ILLUSTRATIONS

CHAPTER 1

INTRODUCTION

In recent years, the gyrotron oscillators[1-3] have been intensively developed and successfully used, for example, for plasma heating experiments.[4] There are many other applications of gyrotrons as high-power microwave and millimeter wave devices. Since amplifiers are in more demand than oscillators for applications to communications, accelerators, and radars, there are various development programs for gyrotron amplifiers such as gyro-klystrons[5] and gyro-TWTs.[6] We observe that virturally all the oscillators in the past have had potential as amplifiers. The electron beam in gyrotrons is hollow, and the individual electron orbit is off-centered, i.e., in a slow-rotational equilibrium about the system axis. Gyrotrons are, therefore, operated by the electron cyclotron maser instability mainly with the axisymmetric modes of a cirular circuit, e.g., the TE_{on}-modes. In other words, the gyrotron is basically a overmoded device, which may not be convenient for use as an amplifier due to mode competition. On the other hand, the dominant mode in a circular waveguide is the TE_{11}-mode whose electric field intensity is peaked on the axis. An axis-rotating beam is, therefore, the most efficient configuration for the excitation of the TE_{11}-mode.[7]

The relativistic axis-rotating electron beams have been produced primarily for plasma confinement[8] and collective ion acceleration.[9] In these devices, powerful microwave radiation was observed, and the interaction mechanism was identified as the negative mass instability.[10-12] The spectrum analysis indicated that the radiation contained many harmonic frequencies simultaneously, i.e., mode competition. Control of this mode competition was reported by employing a multivane circuit, which could provide a preferential azimuthal harmonic number of the radiation fields in the circuit corresponding to the number of vanes.[13] The first attempt to develop a practical microwave device using a non-relativistic electron beam was the cusptron microwave tube.[14]

One of the simple ways of producing axis-rotating beams is the use of an axial cusp magnetic field, into which a hollow beam is injected. After the cusp transition, the hollow beam becomes an axis-rotating electron beam (E layer), which propagates downstream. An axis-rotating beam is bunched azimuthally by the negative mass instability, and the beam energy is thereby transferred into the wave energy. This azimuthal beam bunching may be compared to the phase bunching in gyrotrons which maintains the annular beam shape in real space. Therefore, the harmonic frequency interaction exists inherently in the cusptron. Many theoretical investigations[7,11,12] were conducted on the TE_{11}-mode interaction with an axis-rotating beam at the fundamental cyclotron frequency. However, there was no experimental investigation of this interaction due mainly to the fact that most of the previous devices[8,9] were not properly designed for the TE_{11} interaction. In this paper, we report a useful interaction of an axis-rotating beam with asymmetric radiation fields, namely the TE_{11}-mode, at the fundamental electron cyclotron frequency. It is free from mode competition and potentially important for amplifier applications.

CHAPTER 2

NEGATIVE MASS INSTABILITY

The negative mass stability properties for the TE waveguide modes have been investigated in Reference 15 for the choice of the electron distribution function in which all electrons have the same energy and the same canonical angular momentum, but a Lorentzian distribution in the axial canonical momentum. In the limit of a smooth conducting wall ($R_a \rightarrow R_c$ in Reference 15), the dispersion relation is considerably simplified. For a tenuous beam, the vacuum TE-mode dispersion relation, $\omega^2/c^2 - k^2 = \alpha^2/R_c^2$ is a good approximation for the TE_{11}-mode, where α is the first root of $J_1'(\alpha) = 0$, and R_c is the waveguide radius. Taylor expanding the dispersion relation in Eq. (28) in Reference 15 about the vacuum TE mode dispersion relation, we obtain

$$\left(\frac{\omega^2}{c^2} - k^2 - \frac{\alpha^2}{R_c^2}\right)\left(\omega - \omega_c - k\beta_z c + i|k|\beta_z c\,\frac{\gamma\hat{\Delta}}{\gamma_z^3}\right)^2$$

$$= 4\,\frac{\nu}{\hat{\gamma}}\,\frac{R_o^2\omega_c^4}{c^2}\left(1 - \frac{k^2c^2}{\omega_c^2}\right)\frac{[J_1'(\alpha R_o/R_c)]^2}{J_1''(\alpha)\,J_1(\alpha)\,R_c^2}\,, \qquad (1)$$

where ν is the Budker's parameter, R_o is the beam radius, ω_c is the electron cyclotron frequency, γmc^2 is the total electron beam energy, and Δ is the half width of the axial momentum spread. From Eq. (1), the lowest order eigenfrequency ω and axial wavenumber k are obtained from the simultaneous solution of the vacuum TE mode dispersion relation and the cyclotron resonance condition. However, defining $\chi = (\omega - \omega_c - k\beta_z c)(\gamma/\nu)^{1/3}/\omega_c$, we can approximate Eq. (1) by

$$\chi^3 = 2\left(\frac{1 - \varsigma^2}{1 + \beta_z\varsigma}\right)\frac{[J_1'(R_o\alpha/R_c)]^2R_o^2}{J_1''(\alpha)\,J_1(\alpha)\,R_c^2}\,, \qquad (2)$$

for $\Delta = 0$. In Eq. (2), $\varsigma = kc/\omega_c$. The dispersion relation of the third order polynomial for χ in Eq. (2) clearly exhibits a strong instability.

CHAPTER 3

EXPERIMENT

The experimental set up is shown schematically in Figure 1. The magnetic cusp field is produced by three independently controlled power supplies to the coils. The cusp transition width is narrowed substantially by an iron plate placed between the coils, C2 and C3. The transition length has been measured as 4.8 mm, which is determined by the Full-Width-Half-Maximum (FWHM) of the radial magnetic field at the opening of the iron plate. The system vacuum is maintained by ion pumps at 1.0×10^{-8} Torr.

A hollow electron beam is produced from an annular thermionic cathode of 1.5 cm radius and 0.2 cm radial thickness with a Pierce-type focusing electrode. An anode with an annular slit supported by three bridges is attached to the iron plate. The annular slit of 0.2 cm width allows the hollow beam to pass through the magnetic cusp transition region, where the ($v_z \times B_r$) force converts the beam axial velocity into the azimuthal velocity in the downstream of the cusp transition.

The downstream cavity is electrically isolated by a 20 cm long ceramic insulator, so that the total beam current delivered to the cavity can be monitored by a pickup loop to the ground lead. The cavity is formed by a stainless steel tube of 7.41 cm radius and 43.5 cm length with a blank flange at the other end. Two RF couplers are installed on the end plate; one at the center and the other at 2.0 cm from the axis. The resonant frequencies of the cavity are exactly measured using these couplers, a calibrated CW sweep oscillator, and a spectrum analyzer. The in situ measurements show 1.243 and 1.363 GHz for the TE_{111} and TE_{112}-modes, respectively. Therefore, the required magnetic fields are approximately 465 and 520 G, respectively, for the fundamental cyclotron interaction by a 30 keV beam without the Doppler shift effect.

The electron gun (diode) is operated by a high-voltage modulator up to 30 kV normally with a perveance of 0.6 μperv. The pulse repetition rate is set at 60 Hz to eliminate the neutralization effect of the background ions and to observe multiple oscilloscope traces constantly. The magnetic field produced by the series connected coils, C2 and C3, mainly controls the cusp transition characteristics of the electron beam. While the magnetic field from the downstream coils controls the resonance condition for the interaction, the first coil, C1, controls the beam launching angle and thereby the interaction intensity. The details of the electron motion in a cusp transition may be found in Reference 16.

A block diagram of the radiation diagnostics is shown in Figure 2. A microwave reflectometer dual directional coupler) is used to divide the signal into a crystal detector, a power meter, and a spectrum analyzer. While the microwave frequency is precisely detected by the spectrum analyzer, the microwave power is carefully determined by calibration of these three instruments. In the calibration, every instrument is fixed including the cables and the control knobs of the instruments. The cable from the RF coupler is disconnected from the cavity and reconnected to a calibrated power source at the observed frequency without the attenuators before the crystal detector. The power measurements from chese instruments are consistent to within ± 10 percent.

The TE_{111} and TE_{112}-modes are separately excited by adjusting magnetic field configurations, and thereby the beam characteristics. The observed frequencies are upshifted by 20-25 MHz from the resonance frequencies obtained from the cold tests. This compares well with the theoretical value of 20 MHz, which is obtained from Eq. (2) for $R_0 = 1.0$ cm and $\beta_z = 0.06$. Typical experimental results for TE_{112}-mode generation are shown in Figures 3 and 4. The top trace in Figure 3 shows the crystal detector signal of 140 mV, which corresponds to the 65 dB-attenuated microwave power of 1.8 kW. The middle trace is the total beam current of 0.8 A delivered to the cavity, and the bottom trace shows the beam energy of 29 keV. In this case, the electronic efficiency is approximately 7.8 percent. The spectrum analyzer trace is shown in Figure 4, where the microwave frequency is 1.384 GHz with less than 1 MHz width at the 3 dB level. The TE_{111}-mode at 1.266 GHz shows similar behavior with a slightly lower efficiency. It is important to note that we have never observed any mode competition in this experiment.

CHAPTER 4

CONCLUSION

In conclusion, the TE_{111} and TE_{112}-modes of a circular cavity are excited separately at the fundamental electron cyclotron frequency by an axis-rotating electron beam of 28-30 keV, 0.8-1.0 A, and 4 μs via the negative mass instability. Radiation power is about 1.8 kW with an approximately 7.8 percent efficiency at 1.266 and 1.384 GHz, respectively. The applied magnetic field in the cavity is in the range of 465-520 G. This experiment has successfully demonstrated that a non-relativistic axis-rotating beam can be used to generate the dominant mode effectively without mode competition. This device holds promise as an efficient oscillator and/or amplifier useful for many important applications.

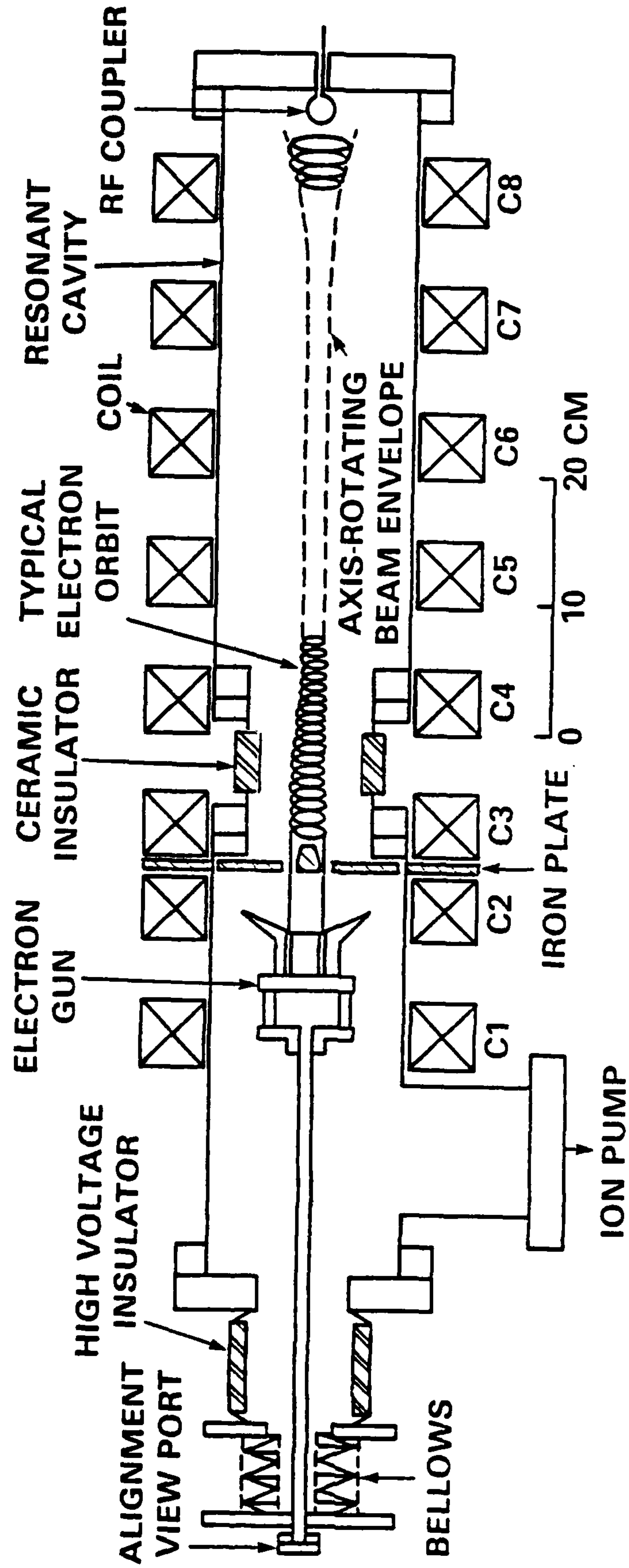

FIGURE 1. SCHEMATIC OF EXPERIMENTAL SETUP

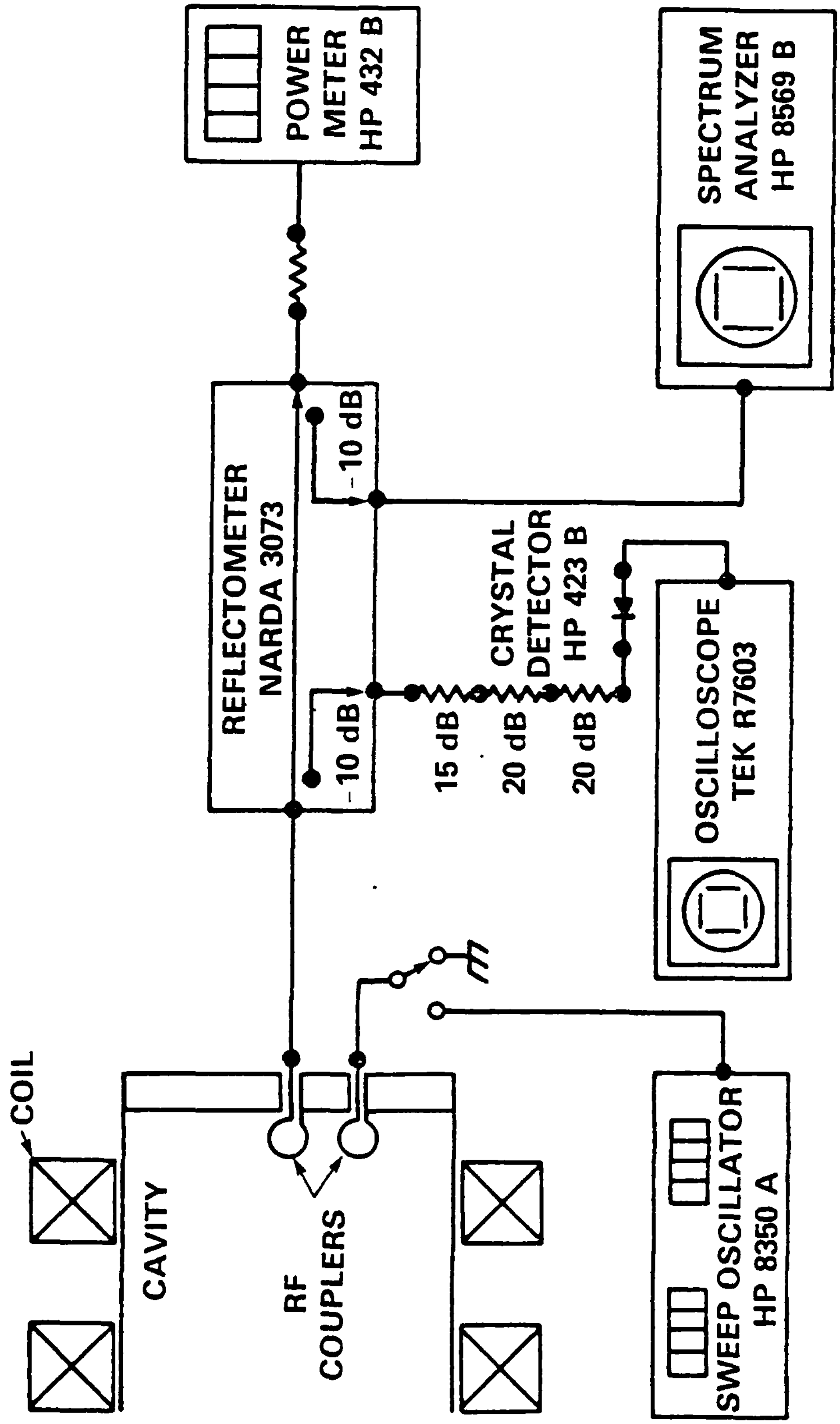

FIGURE 2. BLOCK DIAGRAM OF RADIATION DIAGNOSTICS

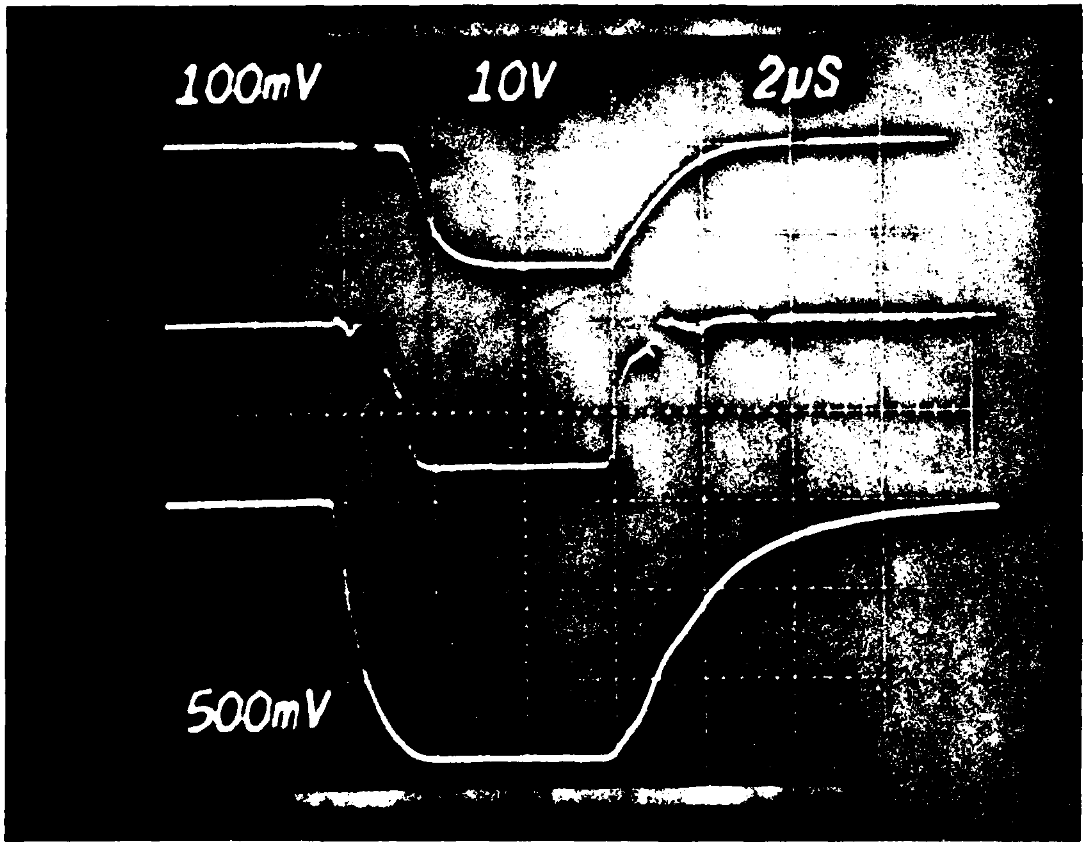

FIGURE 3. TYPICAL OSCILLOSCOPE TRACES FOR TE_{112}-MODE GNERATION (TOP TRACE IS 65 dB-ATTENUATED DETECTOR SIGNAL OF 140 mV (100 mV/DIV) CORRESPONDING TO RADIATION POWER OF 1.8 kW, MIDDLE TRACE FOR BEAM CURRENT OF 0.8 A (0.5 A/DIV), AND BOTTOM TRACE FOR BEAM ENERGY OF 29 keV (10 keV/DIV))

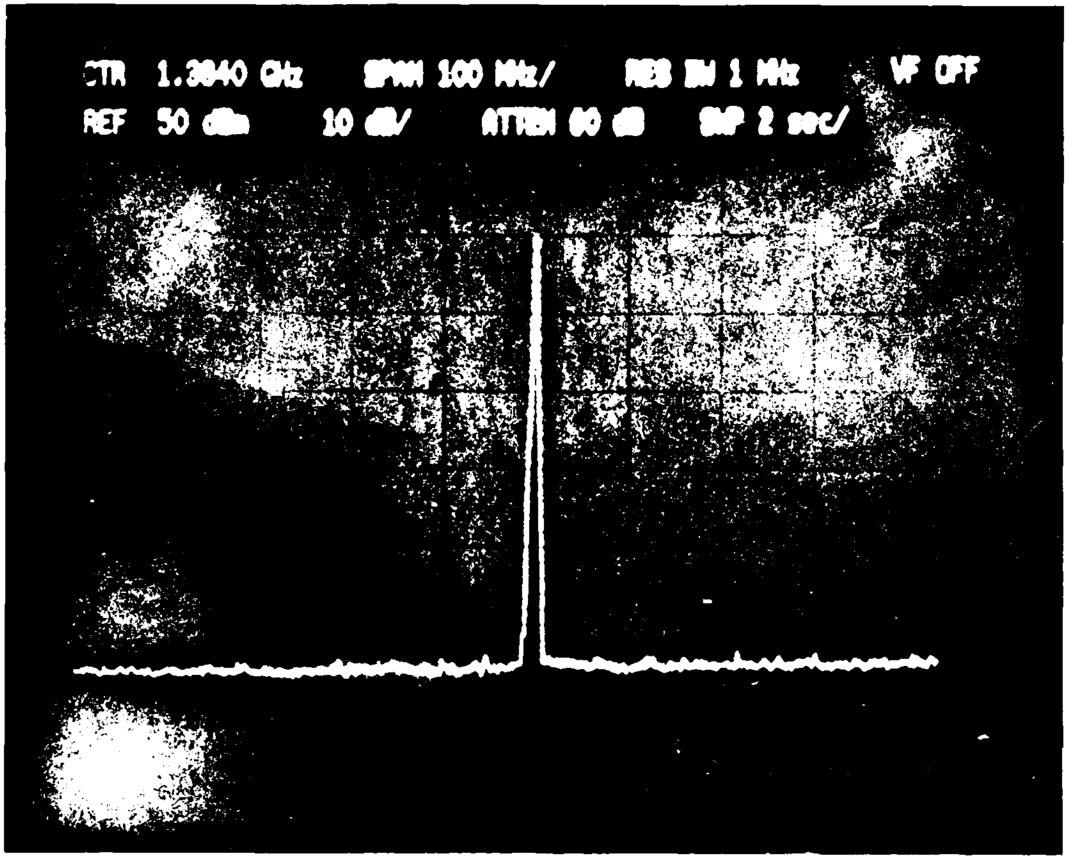

FIGURE 4. SPECTRUM ANALYZER TRACE FOR TE_{112}-MODE GENERATION (CENTER FREQUENCY IS 1.384 GHz WITH 100 MHz/DIV and 10 dB/DIV)

REFERENCES

1. Flyagin, V. A., Gapanov, A. V., Petelin, M. I., and Yulpatov, V. K. IEEE Transactions on Microwave Theory and Technology, Vol. MTT-25, 1977, p. 514.

2. Hirschfield, J. H. and Granatstein, V. L., IEEE Transactions on Microwave Theory Technology, Vol. MTT-25, 1977, p. 528.

3. Uhm, H. S., Davidson, R. C., and Chu, K. R., Physics of Fluids, Vol. 21, 1978, p. 1877.

4. Gilgenbach, R. M., Read, M. E., Hackett, K. E., Lucey, R., Hui, B., Granatstein, V. L., Chu, K. R., England, A. C., Eldridge, O. C., Howe, H. C., Kulchar, A. G., Lazarus, E., Murakami, M., and Wilgen, W., Physical Review Letters, Vol. 44, 1980, p. 650.

5. Bollen, W. M., McCurdy, A. H., Arfin, B., Parker, R. K., and Ganguly, A. K., IEEE Transactions on Plasma Science, Vol. PS-13, 1985, p. 417.

6. Park, S. Y., Vanderplatts, N., Ahn, S. Y., Ganguly, A. K., Parker, R. K., and Granatstein, V. L., IEEE Transactions on Plasma Science, Vol. PS-13, 1985, p. 404.

7. Choe, J. Y. and Ahn, S., IEEE Transactions on Electron Devices, Vol. ED-28, 1981, p. 94.

8. Christofiolos, N. C., Briggs, R. J., Hester, R. E., and Weiss, P. B., Proceedings of Conference on Plasma Physics and Controlled Nuclear Fusion Research (IAEA, Vienna), Vol. 2, 1966, p. 211.

9. Destler, W. W., Hudgings, D. W., Rhee, M. J., Kawasaki, S., and Granatstein, V. L., Journal of Applied Physics, Vol. 48, 1977, p. 3291.

10. Nielson, C. E., Sessler, A. M., and Symmon, K. R., in Proceedings of International Conference on High-Energy Acclerators and Instrumentation, CERN, Geneva, Switzerland, 1959.

11. Sprangle, P., Journal of Applied Physics, Vol. 47, 1976, p. 2935.

REFERENCES (Cont.)

12. Uhm, H. S., and Davidson, R. C., Journal of Applied Phyics, Vol. 49, 1978, p. 593.

13. Destler, W. W., Weiler, R. L., and Striffler, C. D., Applied Physics Letters, Vol. 38, 1981, p. 570.

14. Namkung, W., Physics of Fluids, Vol. 27, 1984, p. 329.

15. Uhm, H. S., Kim, C. M., and Namkung, W., Physics of Fluids, Vol. 27, 1984, p. 488.

16. Rhee, M. J., and Destler, W. W., Physics of Fluids, Vol. 17, 1974, p. 1574.

DISTRIBUTION

	Copies
Defense Technical Information Center Cameron Station Alexandria, VA 22314	12
Library of Congress Attn: Gift and Exchange Div. Washington, DC 20504	4
Strategic Defense Initiative Organization	
Attn: IST (H. E. Brandt)	1
DEW (R. Gullickson)	1
Washington, DC 20301-7100	
Commander Naval Research Laboratory	
Attn: Code 6840 (R. Parker)	1
Code 4740 (W. Manheimer)	1
Code 4790 (P. Sprangle)	1
Code 4704 (J. Golden)	1
Washington, DC 20375	
Massachusetts Institute of Technology	
Attn: R. C. Davidson	1
G. Bekefi	1
R. Temkin	1
Plasma Fusion Center 77 Massachusetts Ave. Cambridge, MA 02139	
University of Maryland	
Attn: W. W. Destler	1
V. L. Granatstein	1
M. J. Rhee	1
Electrical Engineering Department College Park, MD 20742	

	Copies
Cornell University	
Attn: J. Nation	1
E. Chojnacki	1
H. Fleischmann	1
Laboratory of Plasma Studies Ithaca, NY 14850	
Internal Distritution:	
D2	1
F40	5
R	1
R01	1
R04	1
R40	1
R401	1
R41 (M. Brown)	1
R41 (R. Chen)	1
R41 (D. Land)	1
R41 (K. Nguyen)	1
R41 (S. Stern)	1
R41 (R. Stark)	1
R41 (R. Schneider)	1
R41 (J. Smith)	1
R41 (H. Uhm)	5
R42	1
R43	1
R43 (V. Ayres)	5
R43 (J. Choe)	5
R43 (W. Namkung)	20
R43 (J. Scarzello)	1
R44	1
R45	1
E231	2
E232	15

END

FILMED

MARCH, 1988

DTIC